

# PATTERNING OF THIN-FILM SILICON MODULES USING LASERS WITH TAILORED BEAM SHAPES AND DIFFERENT WAVELENGTHS

S. Haas<sup>#</sup>, S. Ku<sup>#○</sup>, G. Schöpe<sup>#</sup>, K. Du<sup>\*</sup>, U. Rau<sup>#</sup>, H. Stiebig<sup>#+</sup>

<sup>#</sup> Institute of Photovoltaics, Research Centre Jülich, D-52425 Jülich, Germany

<sup>○</sup> Department of Physics, Shanghai Jiao Tong University, 200240 Shanghai, China

<sup>\*</sup> EdgeWave GmbH, Schumanstraße 18b, D-52146 Würselen, Germany

<sup>+</sup> Malibu GmbH & Co. KG, Böttcherstraße 7, D-33609 Bielefeld, Germany

**ABSTRACT:** A detailed analysis of the front contact ablation step and the silicon ablation process for the fabrication of the series interconnection of thin-film silicon modules in superstrate configuration is presented. In this study pulsed lasers with wavelengths of 355 nm and 532 nm were used. The front contact ablation was investigated for zinc oxide as well as for tin dioxide applying an UV-laser from the glass side. As measure of the quality the achieved separation resistance and line profile measurements were used. The silicon ablation step is studied by a green laser with a two dimensional Top-Hat profile. Here the quality of the process was mainly assessed by the contact resistance between front and back contact.

**Keywords:** Thin Film, a-Si:H, Laser Processing

## 1 INTRODUCTION

The cost reduction of solar generated electricity is one of the greatest challenges of the solar business. Therefore technologies with a high cost reduction potential are needed, like thin-film silicon technology. Thin-film technologies in general are one of the most promising candidates to achieve a significant cost reduction in the near future, since most of them offers several advantages compared to the well-established wafer based technology like a much lower material consumption, the possibility of large area deposition, low temperature processes, use of cheap and flexible substrates, and the integrated series connection. Unlike the CdTe and CI(G)S technology the silicon approach can take benefit from the well established production equipment for thin-film transistors in the flat panel display market. Moreover, the production process of this technology is environment-friendly and non-toxic materials which are abundantly available are used. For tandem cell structures based on amorphous (a-Si:H) and microcrystalline silicon ( $\mu$ c-Si:H) initial module efficiencies of 13.4 % and stable module efficiencies exceeding 10 % have already been achieved [1-3]. Furthermore, initial cell efficiencies of 15 % are reported for triple-junction solar cells based on a-Si:H and  $\mu$ c-Si:H and their alloys [3, 4].

Thin-film silicon modules are usually fabricated by an alternating sequence of layer deposition and layer patterning steps, whereas the resulting device consists of serially connected cell stripes. Here all patterning steps can be performed by means of laser scribing processes. In contrast to other patterning techniques like a lift off process or mechanical scratching, laser scribing offers a high throughput and a small area loss. Moreover laser systems are well integrable in automatic production processes, so that a high degree of automation for the module fabrication can be obtained.

Usually Q-switched, single-mode lasers (TEM<sub>00</sub>) with circular Gaussian beam shapes are used for patterning of thin-film silicon modules in superstrate configuration [5]. For the patterning of the transparent conductive oxide (TCO) the commonly used approaches are a near infrared laser ( $\lambda = 1064$  nm) applied from the

glass side [5] or an UV laser ( $\lambda = 355$  nm) applied from the film side [6]. In contrast we have investigated this patterning step applying an UV laser from the glass side, since this can combine the advantages of both commonly used approaches. First the absorption of TCO's is typically higher in the UV wavelength range compared to the absorption in the near infrared. Second the energy is mostly absorbed at the glass-TCO interface where the TCO should be cleanly ablated. Furthermore we investigated a special approach for the silicon layer ablation. Usually a green laser ( $\lambda = 532$  nm) with a circular beam characteristic is used for this step [5]. We investigated the application of a Q-switched slab laser with a rectangularly shaped two dimensional Top-Hat beam profile. This profile has several advantages. The energy efficiency is much higher, since the fraction of the laser power density which is under the ablation threshold of the silicon is much lower compared to Gaussian beams. Furthermore the ablation area is irradiated by nearly constant laser intensity. Thus an inhomogeneity in the ablation area can be almost avoided.

In section 2.1 the different patterning processes that are necessary for the silicon thin-film module production are briefly introduced and the patterning steps investigated in this work are specified. The experimental setup at our institute is described in section 2.2. In section 3.1 the results achieved for the TCO ablation with an UV laser applied from the glass side are discussed. Section 3.2 describes the findings of the silicon patterning with a two dimensional Top-Hat beam.

## 2 EXPERIMENTAL

### 2.1 Patterning process

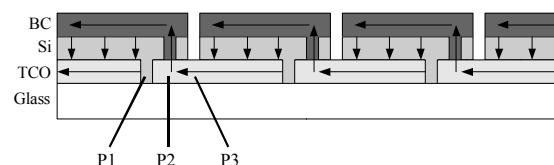


**Figure 1:** Schematic drawing of a thin-film silicon module. P1 - P3 indicates the different patterning steps.

Figure 1 shows a schematic drawing of a thin-film silicon module in superstrate configuration. The arrows indicate the photocurrent of an illuminated module under short circuit conditions. Through the patterning process the individual layers – TCO (P1), silicon thin film layer stack (P2), and back contact system (P3) – are selectively removed. Thus, the total area of the module is divided into serially connected cell stripes. Details regarding the integrated series connection are given elsewhere [7].

As mentioned above the investigation of the front contact ablation was concentrated on the application of an UV laser. Several samples with different types of TCO have been used, as listed below.

**Table I:** Samples used for the investigation of the front contact ablation with an UV laser

|                          | In house | AFG              | LOF              | AsahiU           |
|--------------------------|----------|------------------|------------------|------------------|
| TCO type                 | ZnO      | SnO <sub>2</sub> | SnO <sub>2</sub> | SnO <sub>2</sub> |
| Sheet resistance [Ω]     | 3.6      | 13.8             | 7.5              | 9                |
| TCO layer thickness [nm] | ~ 820    | ~ 950            | ~ 650            | ~ 1200           |
| Type of glass            | white    | green            | green            | green            |
| Glass thickness [mm]     | 1.1      | 3.2              | 3.0              | 1.1              |

The samples were irradiated from the glass side. For the investigations a lens with a focal length of 100 mm was used. The laser power  $P$  was varied in a range of 80 mW to 950 mW which corresponds to a pulse energy  $E_{\text{pulse}}$  of 5.3 μJ to 63.3 μJ. The pulse repetition frequency  $f$  was kept constant at 15 kHz. The feed rate  $v$  was adapted between 100 mm/s and 700 mm/s to produce non-stop laser lines with low pulse overlap. The adaptation of the feed rate is necessary since an increase of the laser power leads to a decreasing ablation area. The quality of the laser lines was analyzed with optical microscopy and depth profile measurements. Additionally the electrical quality of the lines was evaluated by measuring the separation resistance of patterned squares with a side length of 5 mm.

The investigations regarding the removal of the silicon layer stack (P2) were carried out on two different kinds of samples with silicon layer thicknesses of 300 nm (a-Si:H) and 1100 nm (μc-Si:H). The a-Si:H samples were deposited on tin-oxide (AsahiU) and the μc-Si:H samples on in house zinc-oxide substrates. Before the laser processing a couple of samples were covered with an additional thin zinc-oxide layer on top of the silicon, to prevent oxidation of the silicon by exposure to air. As back contact a thermally evaporated silver layer was used with a total thickness of around 700 nm. It was deposited after the ablation of the silicon. The ablation has been carried out by a green laser applied from the glass side with a wavelength of 532 nm. This offers the possibility of a selective removal of the silicon, since the underlying TCO is very transparent in this wavelength range. For the investigations a lens with a focal length of 70 mm was used. The laser power  $P$  was varied in a range of 34 mW

to 1300 mW at a constant pulse repetition frequency  $f$  of 10 kHz. This corresponds to pulse energies  $E_{\text{pulse}}$  of 3.5 μJ to 130 μJ. The used feed rate  $v$  was 250 mm/s for  $P = 34 \text{ mW} - 60 \text{ mW}$  and 400 mm/s for  $P = 120 \text{ mW} - 1300 \text{ mW}$ . The laser used for the investigation was supplied by EdgeWave GmbH, Germany. It has a slab-shaped laser crystal which offers several advantages. The special design of the slab laser crystal allows for an effective cooling since thermally contacted heat sinks can be directly mounted on two optically inactive large faces of the crystal. Furthermore the short resonator design of the laser results in short pulse durations (~ 15 ns) and the laser source offers a nearly two dimensional Top-Hat beam profile. The main focus of the investigations was put on the optimization of the contact resistance between front and back contact (see fig. 1). The contact resistance was calculated by transmission line measurements, which are explained in detail in reference [8]. The measurements have been performed in a voltage range between -0.4 V and 0.4 V with a step size of 0.05 V. The laser line length was always 1 cm. Additionally the quality of the laser scribing process was analyzed by optical microscopy and scanning electron microscopy (SEM).

## 2.2 Experimental setup

The patterning system at our institute consists of several neodymium-doped solid state lasers. The diode pumped laser sources emit pulses (Q-switched) with a wavelength of  $\lambda = 1064 \text{ nm}$  (IR laser), frequency doubled with a wavelength of  $\lambda = 532 \text{ nm}$  (green lasers) or frequency tripled with a wavelength of  $\lambda = 355 \text{ nm}$  (UV laser). All lasers excepting the Top-Hat system operate in TEM<sub>00</sub> mode. The pulse durations measured (full-width at half-maximum) are between  $\tau_{\text{pulse}} = 10\text{-}20 \text{ ns}$  for all lasers. For the measurement of the laser pulse durations a fast photodiode in combination with a LC684DXL scope from LeCroy was used. The repetition frequency  $f$  of the laser pulses can be varied over a wide range ( $0 \text{ kHz} < f < 100 \text{ kHz}$ , depending on the used laser). The laser power  $P$  is usually adjusted through the excitation current of the respective pump source. Only the output power of the UV laser is adjusted by an external attenuator. This has the advantage that the laser source itself can work in optimized, stable conditions. For positioning of the laser beam a split-axis-system is used that allows patterning in a horizontal plane. Linear motors with a maximum feed rate  $v$  of 1000 mm/s drive both horizontal axes. The laser spot can be positioned with accuracy in the micrometer range. Different focusing lengths between 70 mm and 300 mm can be used. The laser beams can be applied from the glass side as well as from the film side.

## 3 RESULTS

### 3.1 TCO patterning by UV irradiation

The patterning of TCO from the glass side combines two advantages of the commonly used approaches as described in the introduction. We found out that for all investigated samples a clear ablation of the TCO material can be achieved without a cracking of the underlying glass substrate. Figure 2 shows exemplary a micrograph of a zinc oxide sample patterned with  $E_{\text{pulse}} = 6 \text{ μJ}$  and  $v = 300 \text{ mm/s}$ . Additionally the depth profile of a line patterned with equal pulse energy is shown.

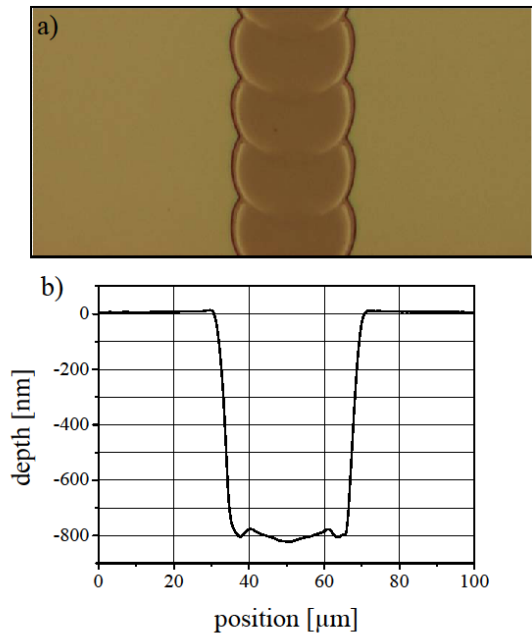


**Figure 2:** Micrograph (a) and depth profile (b) of patterned ZnO. In both cases the TCO was ablated with a diode pumped UV laser with a pulse energy of  $6 \mu\text{J}$ .

The figure shows that a clear ablation is possible also for very low laser intensities. In contrast to the prior investigated TCO ablation with a diode pumped IR laser [9], no cracks were observed in the vicinity of the line. Furthermore the TCO lift-off from the substrate at the line border is much less pronounced compared to the results achieved with the IR laser. The separation resistance of the sample is larger than  $20 \text{ M}\Omega$ . The clear ablation of the zinc oxide is due to the much higher absorption of laser beams with a wavelength of  $355 \text{ nm}$  compared to beams with a wavelength of  $1064 \text{ nm}$  [9]. In the near IR the outer area of a Gaussian laser beam is not sufficient for a clear ablation, it just leads to a heating of the periphery of the ablated area. In contrast for the UV range much lower laser intensity is sufficient for a clear ablation. Thus the outer area of the beams leads also to a clear ablation without significant heating of the periphery of the ablated area. Another indication for this behavior is the comparable width of the UV produced lines and the IR produced lines, although the spot size of the UV beam is lower in the focal plane. For an increase of the pulse energy the feed rate can be also increased up to  $600 \text{ mm/s}$  at constant repetition frequency without any decrease of the separation resistance. For higher feed rates the resistance drops abruptly, since the individual laser spots are no longer connected. Nevertheless higher repetition frequencies should in principal allow higher feed rates without a drop of the separation resistance. A further important property is that a cracking of the substrate glass did not occur also for high laser powers and high feed rates.

For the other investigated types of TCO similar results were achieved. A clear ablation was already obtained for low pulse energies in the range of  $6 \mu\text{J}$  –  $12.6 \mu\text{J}$  although several glass substrates are much thicker and thus the absorption of the UV light in the glass is much higher compared to absorption in the glass of the ZnO substrate (see tab. 1). Here the separation

resistances are always above  $20 \text{ M}\Omega$ . With increasing pulse energy the feed rate could also be increased without a decrease of the separation resistance up to velocities of  $550 \text{ mm/s}$  –  $600 \text{ mm/s}$ , depending on the used sample. Compared to the IR wavelength range the necessary pulse energies for a clear and highly resistive ablation are much lower in the UV. In the IR range pulse energies of  $150 \mu\text{J}$  to  $200 \mu\text{J}$  are typically used for laser lines with a similar width.

### 3.2 Patterning of the silicon layer stack

#### 3.2.1 Patterning of $\mu\text{c-Si:H}$

For the patterning of the microcrystalline samples the applied laser ablation process produced lines with a width of around  $36 \mu\text{m}$  –  $54 \mu\text{m}$ . With increasing laser intensity the width increases, too. The contact resistance for these samples is shown in figure 3 a as a function of the applied laser power.

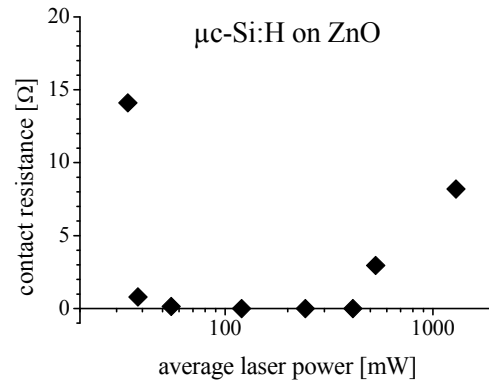


**Figure 3:** Contact resistance of the  $\mu\text{c-Si:H}$  samples deposited on zinc oxide substrates as a function of the applied laser power

The figure clearly shows that the value of the resistance strongly depends on the applied laser power. However for an optimized silicon ablation process the average laser power can be varied over one order of magnitude ( $50 \text{ mW} < P < 400 \text{ mW}$ ) without a dramatic increase of the resistance. In the low power range the increase is a result of an insufficient ablation of the silicon layer stack, most of the material is still left. Small holes occur at irregular distances in the silicon which leads to the remained conductivity. Although the contact resistance of the laser lines scribed with an average laser power of  $P = 120 \text{ mW}$  and above is negligible small, a damage of the TCO material was already observed. However, without a silicon layer stack on top of the TCO, no damage to the TCO was determined for this laser power. Therefore, we identify heat generation during the silicon ablation process as the most probably cause for damage. Figure 4 shows a micrograph of a laser line scribed with an average power of  $120 \text{ mW}$ . The picture is taken from the film side after the silver layer deposition.

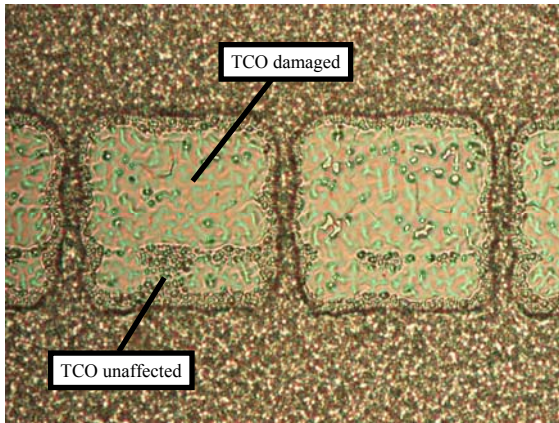


**Figure 4:** Micrograph of a  $\mu\text{-Si:H}$  samples deposited on a zinc oxide substrate patterned with  $P = 120 \text{ mW}$ .

In the upper part of the laser line, the TCO seems to be melted during the ablation process. The fine structure of the TCO topology is disappeared. In the lower part and at the border of each laser spot the TCO is partially unaffected.

For an average laser power of 530 mW and above the contact resistance increases again. This is most probably due to a stronger damage of the TCO; a significant amount of TCO can even be removed during the silicon ablation process.

### 3.2.2 Patterning of a-Si:H

For the amorphous samples the applied laser ablation process produced lines with a width of around  $34 \mu\text{m} - 54 \mu\text{m}$ . With increasing laser intensity the width increases, too. The contact resistance for these samples is shown as a function of the applied laser power in figure 5.

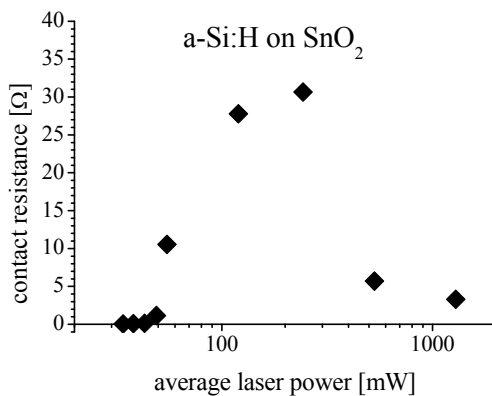


**Figure 5:** Contact resistance of the a-Si:H samples deposited on tin dioxide substrates as a function of the applied laser power

Here the behavior of the contact resistance is completely different compared to the microcrystalline samples. Only for a very narrow process window in the lower power range a good transition between front contact and back contact could be achieved. This characteristic is comparable to the one that was found for a-Si:H on tin dioxide patterned with Gaussian beam shapes [9].

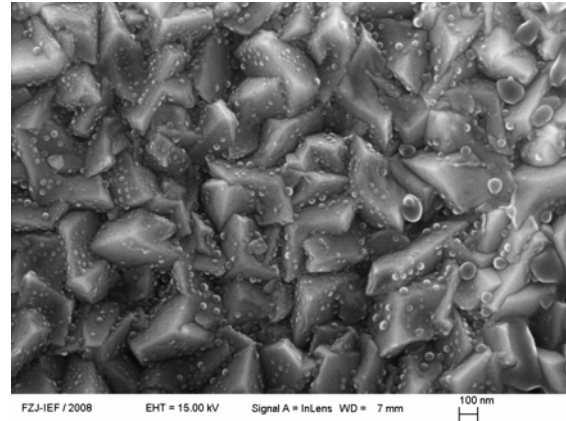


**Figure 6:** SEM picture taken from the bottom of a line patterned with an average power of 34 mW (a-Si:H). Only a small part of the tin dioxide is still covered with little spheres.

Figure 6 shows an SEM picture of an a-Si:H sample on tin dioxide. The picture shows the bottom of a laser scribed line with “good” conditions. The line was patterned with an average laser power of 34 mW. Only a small fraction of the TCO is still covered with little spheres. The spheres may be formed from molten silicon, which indicates that the temperature at the TCO silicon interface must have been above the melting point of silicon. But since the non coated part dominates the surface the contact resistance is very low.

In contrast to the samples patterned with low intensity, the samples with high intensity ( $P > 50 \text{ mW}$ ) show a lot of irregularities in the laser line.

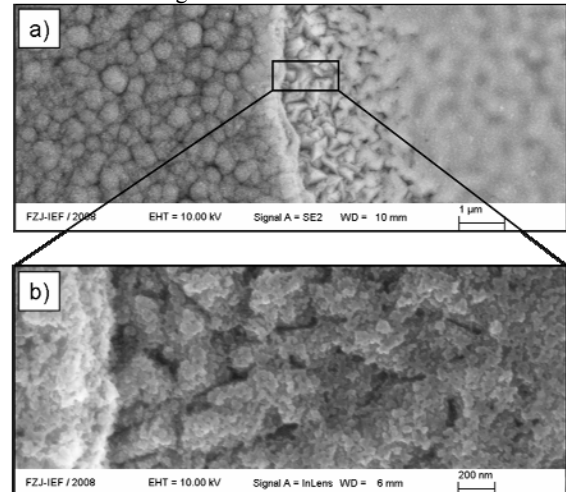


**Figure 7:** SEM picture taken from the edge of a line patterned with an average power of 243 mW (a). Additionally a part of the line near the border is shown with a higher resolution (b). Here a significant amount of residuals are visible.

Figure 7 shows an SEM picture taken from a sample patterned with “bad” conditions. In the center of the laser line most of the TCO material has been molten (Fig. 7 (a), right side). Most probably this leads here to a high contact resistance, although this effect seems to have no influence on the microcrystalline samples deposited on zinc oxide. Whether this difference is due to the different silicon structure or due to the other TCO material used is still under investigation. At the border of the laser line,

where the surface structure of the TCO is still intact, the surface is covered by a continuous layer (Fig. 7 (b)). The resulting topology looks like a coral structure. Also this layer seems to inhibit the current flow. For very high laser powers ( $P = 530$  mW and above) the contact resistance drops again. But it never reaches the values of the samples patterned at low power. In this high power region most of the TCO material is removed during the silicon ablation.

#### 4 CONCLUSUION

A detailed analysis of the front contact ablation step and the silicon ablation process for the fabrication of the series interconnection of thin-film silicon modules in superstrate configuration was presented. For the front contact ablation an UV laser applied from the glass side was used. Compared to the application of IR lasers the UV laser has some advantages, since high separation resistances and clear ablation results without any debris or cracks are achieved for a large pulse energy range.

The silicon ablation step was carried out using a green laser with a Top-Hat beam profile. The influence of the laser power on the quality of the silicon ablation process was mainly analyzed by means of contact resistance measurements. For microcrystalline silicon deposited on zinc oxide a very large process window was found where the laser power could be varied over almost one order of magnitude. For amorphous silicon deposited on tin dioxide the process window is very narrow. Only for laser powers slightly above the ablation threshold of the material a good contact resistance was achieved.

#### ACKNOWLEDGEMENTS

The authors would like to thank Egbert Wessel for his contribution to this work.

#### REFERENCES

- [1] Yamamoto, K., A. Nakajima, M. Yoshimi, T. Sawada, S. Fukuda, T. Suezaki, M. Ichikawa, Y. Koi, M. Goto, T. Meguro, T. Matsuda, M. Kondo, T. Sasaki, Y. Tawada: A Thin film silicon solar cell and module. In: Progress in Photovoltaics: Research and Applications, p. 489-494, 2005
- [2] Repmann, T., B. Sehrbrock, C. Zahren, H. Siekmann, J. Müller, B. Rech, W. Psyk, R. Geyer and P. Lechner: Thin film solar modules based on amorphous and microcrystalline silicon. In: Proceedings of the 3rd World Conference on Photovoltaic Energy Conversion, p. 1574-1579, 2003
- [3] Susumu, F., K. Yamamoto, A. Nakajima, M. Yoshimi, T. Sawada, T. Suezaki, M. Ichikawa, Y. Koi, M. Goto, T. Meguro, T. Matsuda, T. Sasaki and Y. Tawada: High efficiency thin film silicon hybrid cell and module with newly developed interlayer. In: Proceedings of the 21st European Photovoltaic Solar Energy Conference, p. 1535-1538, 2006
- [4] Baojie, Y., G. Yue, J. M. Owens, J. Yang and S. Guha: Over 15% Efficient Hydrogenated Amorphous Silicon Based Triple-Junction Solar Cells Incorporating Nanocrystalline Silicon. In: Proceedings of the 4th IEEE World Conference on Photovoltaic Energy Conversion, p. 1477-1480, 2006
- [5] Haas, S., A. Gordijn, H. Stiebig: High speed laser processing for monolithical series connection of silicon thin-film modules. In: Progress in Photovoltaics: Research and Applications 16, 195 (2008)
- [6] Oerlikon solar: Dream start for micromorph tandem. In: Newsletter 3/2007, [www.oerlikon.com/solar](http://www.oerlikon.com/solar)
- [7] Gupta, Y., H. Liers, S. Woods, S. Young, R. DeBlasio and L. Mrig: Optimization of a-Si Solar Cell Current Collection. In: Proceedings of the 17th European Photovoltaic Specialist Conference, p. 1092-1101, 1982
- [8] Reeves, G. K. and H. B. Harrison: Obtaining the Specific Contact Resistance from Transmission Line Model Measurements. In: IEEE Electron Device Letters Vol. 3, p. 111 - 113, 1982
- [9] Haas, S., A. Gordijn, G. Schöpe, B.E. Pieters and H. Stiebig: Influence of the laser parameters on the patterning quality of thin-film silicon modules. In: SPIE Conference Proceedings Optics and Photonics 2007, San Diego